24 December 1999

ELSEVIER

Chemical Physics Letters 315 (1999) 257–265

CHEMICAL PHYSICS LETTERS

www.elsevier.nl/locate/cplett

Binding of ammonia to small copper and silver clusters

Wai-To Chan, René Fournier *

Department of Chemistry, York University, Toronto, Ontario M3J 1P3, Canada

Received 9 July 1999; in final form 5 October 1999

Abstract

We report equilibrium geometries, harmonic frequencies, and thermochemical data for the metal cluster–ammonia complexes $Ag_n(NH_3)$ and $Cu_n(NH_3)$ ($n = 1,2,3,4$), $Ag_4(NH_3)_2$, and $Cu_4(NH_3)_2$ calculated by a density functional method. The calculated shifts in ammonia umbrella mode frequency correlate with the observed shifts and the calculated enthalpies of complexation. The preferred site for NH_3 adsorption and the calculated bond enthalpies can be rationalized by considering atomic charges obtained from a natural population analysis and polarization of the metal electron density.

1. Introduction

Silver clusters have recently been studied with experiments probing the size dependence of reactivity towards ammonia. Rayner et al. have reviewed enthalpy and entropy changes for NH_3 adsorption on metal clusters of varying size and spectroscopic data of metal cluster–ammonia complexes [1]. Detailed interpretation of experiments for structure elucidation and for a fuller understanding of the reactivity of these clusters requires correlation of experimental and theoretical results. This prompted us to study the ammonia complexes of silver clusters Ag_n ($n = 1,2,3,4$) by density functional theory (DFT). We also studied the corresponding copper cluster series in order to gain more insight into the physical chemistry of these systems. Our copper cluster calculations may also help understand some aspects of ammonia adsorption on copper surfaces, a system that is currently the subject of experimental interest [2]. The number of electrons and importance of electron correlation in transition-metal clusters make DFT a natural choice. We tried various combinations of functionals, basis set, and effective core potential. In Section 2, we assess the accuracy of the method that we chose by comparing our calculations to structural, spectroscopic and thermochemical experimental data. This establishes a procedure which, we think, can provide reliable quantitative predictions in future computational investigations of larger clusters.

2. Methods and background information

Calculations were performed with GAUSSIAN 98 [3]. We chose the DFT functional specified by the keyword B3P86 for most calculations. This method combines Becke's three-parameter hybrid exchange functional [4] with Perdew's gradient-corrected cor-

* Corresponding author. Fax: +1-416-736-5936; e-mail: renef@yorku.ca

0009-2614/99/$ - see front matter
PII: S0009-2614(99)01195-1

Table 1
Equilibrium bond lengths (Å), binding energies (eV), and harmonic vibrational frequencies (cm^{-1}) for copper and silver dimer

Method	Cu_2			Ag_2		
	R_e	D_e	ω	R_e	D_e	ω
B3P86/DZVP	2.264	1.65	235	2.655	1.38	157
BP86/SDD	2.222	2.13	274	2.567	1.72	189
B3P86/SDD	2.224	1.92	271	2.562	1.59	191
Expt.*	2.220	2.01	266.4	2.53	1.66	192.4

* Experimental data for Cu_2 taken from Ref. [14] and data for Ag_2 from Ref. [9].

relation functional [5]. Our choice is motivated partly by the good results obtained with a similar functional – Becke's 1988 exchange [6] with Perdew's 1986 correlation [5] – in recent studies of complexes of copper [7,8] and silver [9] clusters, and partly by practical considerations: inclusion of Hartree–Fock exchange in the hybrid functional makes SCF convergence easier by increasing slightly the small HOMO–LUMO gap of metal clusters [10]. Furthermore, the hybrid B3LYP method yielded accurate dipole moments and infrared (IR) intensities in general [13], and accurate dipole polarizabilities in metal clusters [12]. As we will show, information on the reactivity of metal clusters can be obtained by analysing related properties – partial atomic charges and Raman intensities. Our preferred method, denoted B3P86/SDD, combines the Stuttgart–Dresden effective core potential (ECP) [11] for Ag and Cu with the D95** basis set for ammonia. The ECP basis set describes explicitly 19 valence electrons by a contracted [6s,5p,3d] basis. The keywords specified in GAUSSIAN 98 jobs are 'B3P86/SDD', and 'extrabasis' to put polarization functions on the ligand and change the ammonia basis from D95 to D95**.

We assessed the performance of the B3P86/SDD method by comparing calculated and experimental spectroscopic constants for Cu_2 and Ag_2 (see Table 1). The B3P86/DZVP method, which uses all-electron calculations with the DGAUSS-DZVP basis set [15], suffers large deviations from experimental values. The two sets of ECP calculations, BP86/SDD and B3P86/SDD, both yield estimates of the metal–metal bond lengths, dissociation energies and harmonic frequencies in close agreement with experiment. This shows the importance of including relativistic effects in Cu and Ag, even if only approximately by using an ECP. The B3P86/DZVP and B3P86/SDD methods are in qualitative agreement for the Raman and IR intensities of M_nNH_3. Hence, all geometry optimizations and harmonic vibrational calculations reported here were performed using the B3P86/SDD (ECP) method.

3. Structures and energetics

We consider the series of reactions

$$M_n + mNH_3 \rightarrow M_n(NH_3)_m,$$

where M = Cu or Ag, and (n,m) are (1,1), (2,1), (3,1), (4,1), and (4,2). The optimized structures are sketched in Figs. 1 and 2, spatial and electronic

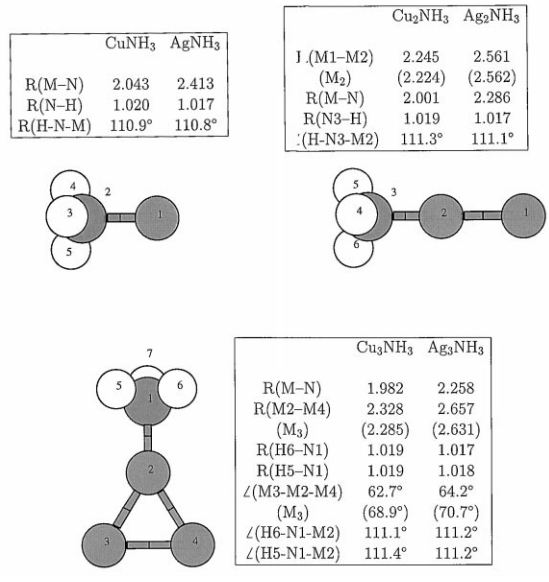

Fig. 1. Structure of the $M_n(NH_3)$ clusters (M = Ag, Cu, and n = 1,2,3) and bond lengths in Å.

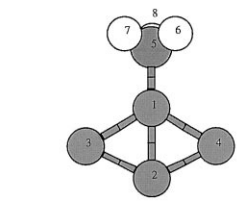

	Cu_4NH_3	Ag_4NH_3
R(M–N)	1.989	2.255
R(M1–M3)	2.449	2.786
(M_4)	(2.394)	(2.743)
R(M3–M2)	2.354	2.708
R(M1–M2)	2.289	2.618
(M_4)	(2.256)	(2.605)
R(N5–H8)	1.019	1.017
R(N5–H7)	1.018	1.017
∠(H8-N5-M1)	110.4°	110.8°
∠(H7-N5-M1)	111.5°	111.1°

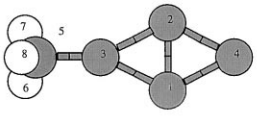

	Cu_4NH_3	Ag_4NH_3
R(M–N)	2.073	2.372
R(M3–M2)	2.434	2.761
R(M2–M4)	2.425	2.769
R(M2–M1)	2.219	2.574
R(N5–H8)	1.019	1.017
R(N5–H7)	1.020	1.017
∠(H8-N5-M3)	111.7°	110.8°
∠(H7-N5-M3)	111.3°	111.1°

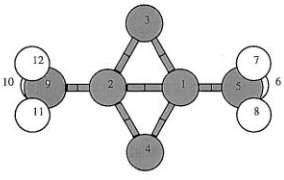

	Cu_4NH_3	Ag_4NH_3
R(M–N)	2.018	2.279
R(M1–M3)	2.400	2.744
R(M1–M2)	2.326	2.629
R(N5–H6)	1.018	1.017
R(N5–H7)	1.018	1.017
∠(H6-N5-M1)	110.2°	110.8°
∠(H7-N5-M1)	111.4°	111.0°

Fig. 2. Structure of the $M_4(NH_3)_m$ clusters (M = Ag, Cu, and $m = 1,2$) and bond lengths in Å.

symmetries are given in Tables 2 and 3. Generally, small ligands can bind 'atop' one atom in the cluster, or to a 'bridge' site with local C_{2v} symmetry, or by capping the center of a M_3 triangular face. For electron–donor ligands, such as NH_3, the atop site is preferred on copper clusters [7] and platinum surfaces [16,17]. Likewise, adsorption of CO to atop sites of small platinum cluster is energetically favoured [18]. We did a few test calculations for adsorption sites other than atop and found that these species relaxed towards the atop geometry upon optimization. In the following, we consider only atop adsorption geometries.

$AgNH_3$ and $CuNH_3$ have C_{3v} equilibrium structures. Their electronic state ($^2A_1$) is non-degenerate and they do not distort to lower symmetry (C_{2v}). The computed Ag–N stretching frequency is in good agreement with the value obtained from the A–X vibronic spectrum of the silver–ammonia stretching [19]. This lends support to assigning $^2A_1$ as the ground state. M_2NH_3 complexes have C_{3v} structures formed by binding the nitrogen end of ammonia to the atop site of the dimer. The equilibrium structure of ground state M_3 was reported to be an obtuse isoceles triangle for copper [22] and silver [9]. Binding NH_3 to M_3 in an atop fashion leads to a C_s symmetry complex where one of the three N–H bond is in a plane perpendicular to the plane defined by M_3 (see Fig. 1). Rotation of NH_3 around the M–N axis gives rise to a C_s geometry where the symmetry plane is coplanar with M_3. The two structures are within 5 cm^{-1} in energy, the torsional rotation of NH_3 is essentially unhindered, and we report only one of the two isomers. Assuming free

Table 2
$Cu_n + NH_3$ adsorption thermochemical data (in kcal/mol, except the energy E (in au) and ΔS (in cal mol^{-1} K^{-1}) at 298.15 K calculated by B3P86/SDD

	Sym	E	ZPE	$-\Delta E_{ad}$	$-\Delta H_{ad}$	$-\Delta S_{ad}$
NH_3	$C_{3v}/{}^1A_1$	−56.7528	21.8			
Cu		−197.7528	0			
$CuNH_3$	$C_{3v}/{}^2A_1$	−254.5291	23.5	13.1	13.7	23.9
Cu_2	$D_{\infty h}/{}^1A_1$	−395.5767	0.4			
Cu_2NH_3	$C_{3v}/{}^1A_1$	−452.3705	24.5	23.5 > 25 [a]	24.1	29.2
Cu_3	$C_{2v}/{}^2B_2$	−593.3682	0.8			
Cu_3NH_3	$C_s/{}^2A''$	−650.1703	25.0	28.4	28.9	26.9
Cu_4	$D_{2h}/{}^1A_1$	−791.2047	1.4			
Cu_4NH_3 (S)	$C_s/{}^1A''$	−848.0052	25.7	27.5	27.9	26.4
Cu_4NH_3 (L)		−847.9832	25.0	14.4	15.1	26.4
$Cu_4(NH_3)_2$	$C_{2v}/{}^1A_1$	−904.7964	49.7	22.0	22.3	30.2

[a] Experimental lower bound; see Ref. [20].

Table 3
$Ag_n + NH_3$ adsorption thermochemical data (in kcal/mol, except the energy E (in au) and ΔS (in cal mol^{-1} K^{-1})) at 298.15 K calculated by B3P86/SDD

	Sym	E	ZPE	$-\Delta E_{ad}$	$-\Delta H_{ad}$	$-\Delta S_{ad}$
NH_3	$C_{3v}/^1A_1$	−56.7528	21.8			
Ag		−147.4205	0			
$AgNH_3$	$C_{3v}/^2A_1$	−204.1873	23.2	7.5	8.1	20.8
Ag_2	$D_{\infty h}/^1A_1$	−294.8995	0.3			
Ag_2NH_3	$C_{3v}/^1A_1$	−351.6821	24.1	16.7	17.2 16.4 ± 3 [a]	27.9
Ag_3	$C_{2v}/^2B_2$	−442.3482	0.5			
Ag_3NH_3	$C_s/^2A''$	−499.1371	24.5	20.6	21.3	29.7
Ag_4	$D_{2h}/^1A_1$	−589.8372	0.9			
Ag_4NH_3 (S)	$C_s/^1A'$	−646.6265	25.0	23.2	21.0 14 [b]	23.6
Ag_4NH_3 (L)		−646.6089	24.5	12.6	10.2	21.7
$Ag_4(NH_3)_2$	$C_{2v}/^1A_1$	−703.4102	48.8	17.3	17.5	29.1

[a] Experimental value from Ref. [21].
[b] Experimental value from Ref. [1].

rotation of the NH_3 group, the symmetry effectively becomes C_{2v}. In the rest of our discussion, existence of multiple rotamers of M_nNH_3 and $M_n(NH_3)_2$ arising from different azimuth orientations of NH_3 is implied although we report a single geometry.

It is well established that the global minimum on the potential energy surface of Ag_4 assumes a D_{2h} rhombic geometry [23,9]. Ligands can bind atop at either the short (S) or long (L) diagonal positions of the rhombus. The two structures are denoted $Ag_4(NH_3)$ (S) and $Ag_4(NH_3)$ (L) in Fig. 2. We also examined NH_3 binding to a higher energy isomer of M_4 formed by atop addition of M to triangular M_3 giving a C_{2v} Y-shaped structure. Ammonia prefers to bind in an atop way to the metal atom which is not in the triangle, the one with lower coordination. However, this structure transforms into the rhombic isomer upon optimization and is excluded from our analysis. Three isomers of $M_4(NH_3)_2$ can be formed by attaching NH_3 to different atop sites: we label them SS, LL, and SL according to the diagonals of the rhombus. We show the most stable isomer $M_4(NH_3)_2$ (SS) in Fig. 2. The LL and SL structures are unstable, they are not minima of the potential energy surface and distort upon geometry optimization.

Our theoretical estimates of enthalpy and entropy changes for adsorption on Cu_n and Ag_n clusters are in Tables 2 and 3. $Ag_2(NH_3)$, $Cu_2(NH_3)$, and $Ag_4(NH_3)$ have been characterized experimentally [1,20]. There are very few possibilities for the structure of $Ag_2(NH_3)$ (and $Cu_2(NH_3)$), and the linear Ag–Ag–NH_3 configuration was established by the agreement of theory and experiment [21]. A comparison of theoretical and experimental estimates of the bond enthalpies of $M_2(NH_3)$ suggests that our calculated bond enthalpies are within a few kcal/mol of the true values and that the lower bounds obtained by the kinetic method of Lian et al. [20] are probably close to actual bond enthalpies. Information on the structure of other $M_n(NH_3)_m$ complexes is not directly available from experiments, therefore we can not definitively assess the accuracy of our calculated bond enthalpy for $Ag_4(NH_3)$.

The enthalpy change for adsorption of a single NH_3 ligand ranges from −14 to −28 kcal/mol for copper clusters, and from −8 to −21 kcal/mol for silver clusters [1]. The strength of the metal–ligand

[1] We estimate the counterpoise correction to basis set superposition error on these values to be less than 1 kcal/mol.

bond is intermediate between strong physisorption and weak chemisorption [2]. Since the Mulliken analysis gives metal–N bond orders smaller than 0.2, the ammonia is best described as 'strongly physisorbed' on the metal clusters. For both series of reactions, ΔH_{ad} increases with cluster size from MNH_3 to M_3NH_3. The calculated ΔH_{ad} for M_3NH_3 and M_4NH_3 (S) are roughly equal. Adsorption of a second NH_3 on M_4NH_3 (S) to give $M_4(NH_3)_2$ (SS) is less exothermic by 4–6 kcal/mol. The entropy change accompanying NH_3 adsorption varies from -20 to -30 cal mol^{-1} K^{-1} for both Cu_n and Ag_n. The large entropy decrease is mainly caused by the loss of the three translational degrees of freedom. These translations become vibrational modes in the complex, resulting in an increase of vibrational entropy that is larger when the vibrational mode frequencies are smaller. Therefore, a relatively small entropy decrease is indicative of a floppy M_nNH_3 complex.

The geometries of the metal clusters change very little upon NH_3 adsorption. Typically, the metal–metal bond lengths increase by 0.05–0.10 Å and the overall structure is retained. Likewise, the geometry of the adsorbed NH_3 ligand is similar to that of the free ligand: the N–H bond lengths increase by less than 0.01 Å and the M–N–H angles are generally within 1° of the pyramidal angle of the free ligand (111.7°). Consistent with this, the structural reorganization energies are very small, less than 0.6 kcal/mol for the M_4 moeity of Cu_4NH_3 and Ag_4NH_3, and essentially zero for NH_3. Nonetheless, we see a correlation between the equilibrium M–N bond length and ΔH_{ad}: R_e (M–N) decreases as binding becomes more exothermic.

The calculated values of ΔH_{ad} and ΔS_{ad} for Ag_2NH_3 agree closely with the experimental values of Ref. [1]. This is reassuring and makes us confident about calculations for complexes that have not been characterized experimentally. The experimental value of ΔH_{ad} for Ag_4NH_3 (-14 kcal/mol) is intermediate between our estimates of -21 kcal/mol for the S structure and -10 kcal/mol for the L structure. The 7 kcal/mol apparent discrepancy between theory and experiment is somewhat surprising. We note, however, that Ag_4 could not be observed because its ionization potential (IP) is too large for photoionization mass spectrometric detection [1]. Our calculated IPs for Ag_4, Ag_4NH_3(S), and Ag_4NH_3 (L) (7.09, 6.56, and 6.22 eV, respectively) raise the possibility that Ag_4NH_3(S) may not have been detected either and that the observed Ag_4NH_3 species may be another isomer, possibly Ag_4NH_3 (L). There is good agreement between B3P86/SDD theory and experiment on the blue shift of the NH_3 inversion (or

[2] See Table 29.1 from *Physical Chemistry*, 4th edn., by P.W. Atkins: the largest enthalpy of physisorption listed for NH_3 is -38 kJ/mol $= 9.1$ kcal/mol.

Table 4
Harmonic frequencies (cm^{-1}), IR intensities (IR, in km/mol) and Raman intensities (Ram, in Å^4/a.m.u.) of Cu_nNH_3 and Ag_nNH_3 ($n = 1,2,3$)

	ω	IR/Ram	ω	IR/Ram
	$CuNH_3$		$AgNH_3$	
M–N str	320 *a*1	3/111	213 *a*1	8/64
NH_3 roc	480 *e*	35/39	213 *a*1	3/37
NH_3 inv	1156 *a*1	142/54	1093 *a*1	153/12
	1650 *e*	26/26	1656 *e*	26/20
sym NH_3 str	3467 *a*1	36/1206	3500 *a*1	9/801
	3615 *e*	30/41	3653 *e*	23/44
	Cu_2NH_3		Ag_2NH_3	
	78 *e*	9/0.8	57 *e*	7/0.3
	243 *a*1	2/37	183 *a*1	0.2/40
M–N str	390 *a*1	12/4	290 *a*1	19/3
NH_3 roc	542 *e*	10/18	495 *e*	17/20
NH_3 inv	1189 *a*1	173/1	1151 *a*1	177/0.1
	1655 *e*	28/9	1659 *e*	27/10
sym N–H str	3493 *a*1	0.2/496	3512 *a*1	0.2/598
	3625 *e*	35/49	3651 *e*	31/57
	Cu_3NH_3		Ag_3NH_3	
Me tor	26 *a*″	0/0.6	19i *a*″	0/0.2
	40 *a*″	2/0.2	13 *a*″	2/0
	78 *a*′	7/0.6	49 *a*′	6/0.2
	152 *a*′	2/4	94 *a*′	1/2
	162 *a*″	4/63	114 *a*″	4/37
	233 *a*′	2/17	168 *a*′	1/18
M–N str	410 *a*′	5/0.7	306 *a*′	11/0.6
NH_3 roc′	561 *a*″	26/36	520 *a*″	38/9
	571 *a*′	16/4	523 *a*′	23/4
NH_3 inv	1205 *a*′	180/4	1171 *a*′	181/6
	1658 *a*″	23/8	1661 *a*′	22/7
	1658 *a*′	30/5	1662 *a*″	22/4
sym N–H str	3501 *a*′	8/185	3517 *a*′	10/234
	3627 *a*′	38/46	3650 *a*′	33/53
	3628 *a*″	33/18	3651 *a*″	30/48

Table 5
Harmonic frequencies (cm^{-1}), IR intensities (IR, in km/mol) and Raman intensities (Ram, in $Å^4$/a.m.u.) of $Cu_n(NH_3)_m$ and $Ag_n(NH_3)_m$ ($n = 4,\ m = 1,2$)

	ω	IR/Ram	ω	IR/Ram
		Cu_4NH_3		Ag_4NH_3
NH_3 tor	43 a''	0.7/1	27 a''	0.4/0.5
	55 a'	1/0.2	36 a'	1/0.1
	69 a''	3/1	40 a''	3/1
	82 a'	7/0.1	51 a'	5/0
	116 a'	4/1	80	3/0.7
	144 a''	0.4/10	99 a''	0.3/8
	154 a'	0.7/23	108 a'	0.3/30
	235 a''	9/0.8	164 a''	7/0.4
	245 a'	0.2/36	179 a'	0.1/30
M–N str	408 a'	4/2	311 a'	8/3
NH_3 roc′	566 a''	10/12	525 a'	19/2
	567 a'	14/2	526 a''	14/8
NH_3 inv	1194 a'	185/3	1162 a'	184/7
	1657 a''	20/7	1660 a''	19/7
	1658 a'	31/4	1661 a'	29/4
sym N–H str	3507 a'	8/156	3521 a'	11/178
	3633 a'	35/39	3654 a'	31/45
	3638 a''	30/20	3657 a''	24/30
		Cu_4NH_3 (L)		Ag_4NH_3 (L)
NH_3 tor	9 a''	0.1/0.6	23 a''	0.3/0
	33 a'	4/4	32 a''	4/3
	33i a''	7/2	33 a'	2/2
	88 a'	4/0.1	64 a'	5/1
	103 a''	0.1/2	71 a''	0.9/0.1
	110 a''	6/0.1	76 a''	4/0
	149 a'	0.3/31	107 a'	0.3/45
	213 a'	12/0.5	155 a'	10/0.7
	284 a'	0.7/24	197 a'	0.2/26
M–N str	313 a'	18/0.5	244 a'	32/4
NH_3 roc′	471 a''	2/13	431 a''	7/15
	488 a'	8/11	436 a'	14/22
NH_3 inv	1172 a'	197/204	1128 a'	204/0.5
	1656 a'	27/3	1658 a''	26/9
	1656 a''	28/3	1659 a'	26/10
sym N–H str	3481 a'	23/1100	3500 a'	11/1829
	3620 a''	26/43	3644 a''	22/84
	3621 a'	28/50	3646 a'	23/94
		$Cu_4(NH_3)_2$		$Ag_4(NH_3)_2$
M–N str′	366 ν_{28} (b_2)	10/0	290 ν_{28} (b_2)	17/0.01
	390 ν_6 (a_1)	0/5	306 ν_6 (a_1)	0/5
NH_3 roc′′′′	525 ν_{13} (a_2)	0/32	495ν_{13} (a_2)	0/20
	529 ν_5 (a_1)	20/2	496 ν_5 (a_1)	33/0.4
	537 ν_{27} (b_2)	0.2/7	501 ν_{27} (b_2)	0/6
	548 ν_{19} (b_1	24/0	513 ν_{19} (b_1)	33/0
NH_3 inv′	1166 ν_{26} (b_2)	416/0.1	1140 ν_{26} (b_2)	405/0.1
	1168 ν_4 (a_1)	0/14	1142 ν_4 (a_1)	0.04/19
sym N–H str′	3506 ν_{24} (b_2)	6/0.1	3521 ν_{24} (b_2)	11/06
	3506 ν_2 (a_1)	0/399	3521 ν_2 (a_1)	0/416

'umbrella') frequency upon complexation (in cm^{-1}): 119 (theory) versus 115 (experiment, Ref. [1]) for Ag_2NH_3; 130 versus a lower bound of 140 for Ag_4NH_3; and 109 versus 115 for $Ag_4(NH_3)_2$. Our calculations show a correlation between the blue shift in inversion mode frequency and binding enthalphy, but no such correlation is apparent among the experimental data [1]. The theoretical values for ΔS_{ad} for structures S and L are similar. The experimental value of ΔS_{ad} is -24 cal mol^{-1} K^{-1} which agrees well with both computed values. Thus, although the calculated enthalpies indicate that Ag_4NH_3 (S) and $Ag_4(NH_3)_2$ (SS) are the thermodynamically favoured isomers, we cannot make a definitive assignment of the observed species.

4. Vibrational modes and spectroscopic properties

The computed harmonic frequencies and IR and Raman intensities for the vibrational modes of the cluster complexes are given in Tables 4 and 5. For $M_n(NH_3)_2$ we show only selected vibrations and label them by the Herzberg order [24]. Vibrations of the NH_3 ligand fall in the 1000–3600 cm^{-1} range and are well separated from the low frequency vibrations in the 20–300 cm^{-1} range characteristic of the metal clusters. Additional vibrational modes in the 0–600 cm^{-1} range arise from binding between M_n and NH_3. In the spectrum of MNH_3 a doubly degenerate rocking mode of NH_3 and a metal–ligand (M–N) stretching mode are observed. In M_2NH_3, degenerate metal–ligand bending modes show up. In addition, binding of NH_3 to a non-linear M_n cluster gives rise to a torsional mode of NH_3 which is found to be the lowest frequency mode. Three of these low frequency vibrational modes are assigned as M–N stretch, NH_3 rocking and NH_3 torsion. Of the modes associated with the NH_3 ligand, we assign only the inversion mode and the totally symmetric N–H stretch. The calculated normal modes of Cu_nNH_3 and Ag_nNH_3 are similar and the energy ordering is the same in the two series. Therefore, we list them together. We get small imaginary frequencies for the NH_3 torsional motion of Ag_3NH_3 and a bending mode of Cu_4NH_3 (L). However, these imaginary frequencies are clearly an artificial result. They are due to small numerical errors which are common in DFT because of the need for numerical integration in calculating some terms of the energy.

Spectroscopic measurement of M_n has focused on the peak corresponding to the NH_3 inversion [1]. Computed *harmonic* frequencies for this mode for Ag_2NH_3, Ag_4NH_3 and $Ag_4(NH_3)_2$ are larger than the observed *fundamentals* (Table 2 of Ref. [1]) by about 5–10% which is reasonable. As we mentioned, there is good agreement between the calculated and observed shift in that mode's frequency relative to free ammonia. We predict a blue shift for the inversion vibration as the size of M_n increases from 1 to 3, and then a red shift by about 10 cm^{-1} for M_4NH_3 (S). The NH_3 rocking mode also shifts to higher frequency as n increases from 1 to 3, and then shifts to lower values for M_4NH_3 (L), but increases for M_4NH_3 (S). Binding of a second NH_3 to M_4NH_3 (S) makes the inversion vibration nearly doubly degenerate, the 'in-phase' (a_1) and 'out-of-phase' (b_2) modes being only 2 cm^{-1} apart. The b_2 peak has a predicted IR intensity twice as large as the single inversion vibration in M_4NH_3.

Raman scattering intensities offer a possible means of structural assignment of M_4NH_3 and $M_4(NH_3)_2$. The most noticeable feature in the computed Raman spectra of $M_n(NH_3)_m$ is a strong Raman signal for

Table 6
Natural population atomic charges for M_4 and M_4NH_3

	Cu_4	Cu_4NH_3 (S)	Cu_4NH_3 (L)	Ag_4	Ag_4NH_3 (S)	Ag_4NH_3 (L)
Q(M1)	+0.279	+.365	+0.248	+0.297	+0.369	+0.270
Q(M2)	+0.279	+.171	+0.248	+0.297	+0.203	+0.270
Q(M3)	−0.279	−0.301	−0.095	−0.297	−0.316	−0.154
Q(M4)	−0.279	−0.301	−0.436	−0.297	−0.316	−0.424
Q(N)		−1.177	−1.196		−1.175	−1.179
$Q(NH_3)$		+0.065	+0.034		+0.061	+0.036

the totally symmetric N–H stretching mode. The Raman intensity of this mode shows a high sensitivity to the metal cluster size and binding site. It is 109 $Å^4$/a.m.u. in free NH_3 and it increases by factors of: 11 on binding to Cu; 7 on binding to Ag; about 5 on binding to either Cu_2 or Ag_2; 10 in Cu_4NH_3 (L) and 17 in Ag_4NH_3 (L), but only about 2 in Cu_4NH_3 (S) and Ag_4NH_3 (S); and 1.5–2 (per NH_3 ligand) in M_3NH_3 and $M_4(NH_3)_2$ complexes. Thus, it may be possible to assign the adsorption site of NH_3 on clusters by looking at ratios of peak intensities. Generally, Raman intensities depend on molecular polarizabilities. For metal clusters, a large intensity enhancement of the symmetric N–H stretch would normally indicate that the metal–N bond is aligned with the longer (more polarizable) axis of the cluster.

5. Further analysis

We now characterize the electron density distribution by examining partial atomic charges obtained from a natural population analysis (NPA) [25] (see Table 6). The NPA has the advantage of having only a small basis set dependence [26]. For Cu_4 and Ag_4, the two atoms at the end of the short diagonal carry positive charges of about $+0.3$ while corresponding negative charges reside on the two atoms of the long diagonal. The N atom carries a negative charge of -1.123 in free NH_3. Binding of NH_3 to Cu_4 or Ag_4 results in a very small transfer of electron (≈ 0.03–0.06) from the ligand to the cluster, but a significant charge redistribution within the cluster. The greater stability of the S isomer of $M_4(NH_3)$ over the L isomer can be understood as due to binding of the *negatively* charged N atom of NH_3 to one of the *positively* charged metal atoms. The NPA charges on atoms M1 and M2 for the S isomer, and atoms M3 and M4 for the L isomer, show that polarization of the metal cluster electron density away from the NH_3 ligand is also an important aspect of the interaction. Because NPA charges can be obtained at a low cost, it may be possible to predict the binding site of NH_3 or similar ligands on large metal cluster without doing many costly cluster–ligand complex calculations. We are currently investigating this possible use of the NPA.

Acknowledgements

Financial support by NSERC Canada and York University is gratefully acknowledged.

References

[1] D.M. Rayner, K. Athenassenas, B.A. Collings, S.A. Mitchell, P.A. Hackett, in: Theory of Atomic and Molecular Clusters with a Glimpse at Experiments, Springer Series in Cluster Physics, Springer, New York, 1999 pp. 371–395, and references therein.
[2] J. Hasselstrom, A. Fohlisch, O. Karis, N. Wassdahl, M. Weinelt, A. Nilsson, M. Nyberg, L.G.M. Petterson, J. Stohr, J. Phys. Chem. 110 (1999) 4880.
[3] GAUSSIAN 98, Revision A.6, M.J. Frisch, G.W. Trucks, H.B. Schlegel, G.E. Scuseria, M.A. Robb, J.R. Cheeseman, V.G. Zakrzewski, J.A. Montgomery Jr., R.E. Stratmann, J.C. Burant, S. Dapprich, J.M. Millam, A.D. Daniels, K.N. Kudin, M.C. Strain, O. Farkas, J. Tomasi, V. Barone, M. Cossi, R. Cammi, B. Mennucci, C. Pomelli, C. Adamo, S. Clifford, J. Ochterski, G.A. Petersson, P.Y. Ayala, Q. Cui, K. Morokuma, D.K. Malick, A.D. Rabuck, K. Raghavachari, J.B. Foresman, J. Cioslowski, J.V. Ortiz, B.B. Stefanov, G. Liu, A. Liashenko, P. Piskorz, I. Komaromi, R. Gomperts, R.L. Martin, D.J. Fox, T. Keith, M.A. Al-Laham, C.Y. Peng, A. Nanayakkara, C. Gonzalez, M. Challacombe, P.M.W. Gill, B. Johnson, W. Chen, M.W. Wong, J.L. Andres, C. Gonzalez, M. Head-Gordon, E.S. Replogle, J.A. Pople, Gaussian, Inc., Pittsburgh, PA, 1998.
[4] A.D. Becke, J. Chem. Phys. 98 (1993) 5648.
[5] J.P. Perdew, Phys. Rev. B. 33 (1986) 8822.
[6] A.D. Becke, Phys. Rev. A 38 (1988) 3098.
[7] R. Fournier, Int. J. Quantum Chem. 52 (1994) 973.
[8] R. Fournier, J. Chem. Phys. 102 (1995) 5396.
[9] R. Poteau, J.-L. Heully, F. Spiegelmann, Z. Phys. D 40 (1997) 479.
[10] G. Valerio, H. Toulhoat, J. Phys. Chem. 100 (1996) 10827.
[11] D. Andrae, U. Haussermann, M. Dolg, H. Stoll, H. Preuss Theor. Chim. Acta. 77 (1990) 123.
[12] P. Fuentealba, Y. Simon, J. Phys. Chem. 101 (1997) 4231.
[13] F. De Proft, J.M.L. Martin, P. Geerlings, Chem. Phys. Lett. 250 (1996) 393.
[14] M.D. Morse, Chem. Rev. 86 (1986) 1049.
[15] N. Godbout, D.R. Salahub, J. Andzelm, E. Wimmer, Can. J. Chem. 70 (1990) 560.
[16] D.R. Jennison, P.A. Schultz, M.P. Schultz, M.P. Sears, Surf. Sci. 368 (1996) 253.
[17] A. Fahmi, R.A. van Santen, Z. Phys. Chem. 197 (1996) 203.
[18] A.M. Ferrari, K.M. Neyman, T. Belling, M. Mayer, N. Rosch, J. Phys. Chem. 103 (1999) 216.
[19] J. Miyawaki, K. Sugawara, H. Takeo, C. Dedonder-Lardeux,

S. Martrenchard-Barra, C. Jouvet, D. Solgadi, Chem. Phys. Lett. 302 (1999) 354.
[20] L. Lian, F. Akhtar, P.A. Hackett, D.M. Rayner, Int. J. Chem. Kin. 26 (1994) 85.
[21] D.M. Rayner, L. Lian, R. Fournier, S.A. Mitchell, P.A. Hackett, Phys. Rev. Lett. 74 (1995) 2070.
[22] C. Massobrio, A. Pasquarello, R. Car, Chem. Phys. Lett. 238 (1995) 215.
[23] V. Bonacic-Koutecky, P. Fantucci, P. Koutecky, Chem. Rev. 91 (1991) 1035.
[24] P.F. Bernath, Spectra of Atoms and Molecules, Oxford University Press, 1995.
[25] A.E. Reed, L.A. Curtiss, F. Weinhold, Chem. Rev. 88 (1988) 899.
[26] C.M. Breneman, K.B. Wiberg, J. Comp. Chem. 11 (1990) 361.